*Journal of Applied Mechanics and Technical Physics, Vol. 45, No. 1, pp. 22–30, 2004*

# ORIGINATION OF MICROCONVECTION IN A FLAT LAYER WITH A FREE BOUNDARY

**V. K. Andreev and E. A. Ryabitskii**

UDC 532.517.013.4

*Stability of a flat layer with a free boundary in the model of microconvection is studied in the linear approximation of equilibrium. The most important physical case is considered, where the Boussinesq parameter and the Rayleigh number depend linearly on the Marangoni number. It is shown that long-wave disturbances always decay. Neutral curves for a wide range of dimensionless parameters are constructed numerically; new (as compared to the Oberbeck–Boussinesq model) growing disturbances are found, which are caused by fluid compressibility. Based on numerical results, the areas of applicability of the microconvection, Oberbeck–Boussinesq, and viscous heat-conducting fluid models are established.*

**Key words:** *microconvection, equilibrium state, free boundary, stability, neutral curve.*

**1. Basic Equations.** The system of equations called the microconvection model in [1] has the following form:

$$\boldsymbol{w}_t + \boldsymbol{w}\nabla\boldsymbol{w} + \beta\chi \operatorname{rot}\boldsymbol{w} \times \nabla\theta + \beta^2\chi^2 \operatorname{div}(\nabla\theta \otimes \nabla\theta - |\nabla\theta|^2 I) = (1+\beta\theta)(-\nabla q + \nu\Delta\boldsymbol{w}) + \boldsymbol{g}; \tag{1.1}$$

$$\operatorname{div}\boldsymbol{w} = 0; \tag{1.2}$$

$$\theta_t + \boldsymbol{w}\cdot\nabla\theta + \beta\chi|\nabla\theta|^2 = (1+\beta\theta)\chi\Delta\theta. \tag{1.3}$$

Here $\beta$ is the coefficient of volume expansion, $\chi$ is the thermal diffusivity, $\otimes$ is the tensor product, $I$ is the unit tensor, $\nu = \mu/\rho_0$ is the kinematic viscosity, and $\boldsymbol{g}$ is the density of external forces. The equation of state of such a fluid is $\rho = \rho_0(1+\beta\theta)^{-1}$, where $\rho_0 > 0$ is a constant. The true velocity vector $\boldsymbol{u}(\boldsymbol{x},t)$ and pressure $p(\boldsymbol{x},t)$ are related to the functions $\boldsymbol{w}(\boldsymbol{x},t)$ and $q(\boldsymbol{x},t)$ as

$$\begin{gathered} \boldsymbol{u} = \boldsymbol{w} + \beta\chi\nabla\theta, \\ p = \rho_0 q + \beta\chi[\lambda + \rho_0(\nu-\chi)]\Delta\theta \end{gathered} \tag{1.4}$$

($\lambda$ is the second viscosity).

It is shown in [1] that the Oberbeck–Boussinesq approximation is invalid for $\eta = l_*^3|\boldsymbol{g}|/(\nu\chi) < 1$, and one should use model (1.1)–(1.3) ($l_*$ is the characteristic scale of the problem).

System (1.1)–(1.3) is supplemented by initial data at $t = 0$

$$\boldsymbol{w} = \boldsymbol{w}_1(\boldsymbol{x}), \qquad \operatorname{div}\boldsymbol{w}_1 = 0, \qquad \theta = \theta_1(\boldsymbol{x}) \tag{1.5}$$

and by the conditions on the solid wall $\Sigma$

$$\boldsymbol{w} + \beta\chi\nabla\theta = 0, \qquad \theta = \theta_\Sigma(\boldsymbol{x},t). \tag{1.6}$$

We assume that $f(\boldsymbol{x},t) = 0$ is the implicit equation of the free boundary $S$. Then, with allowance for substitution (1.4), the following relations are valid on this boundary [2]:

---

Institute of Computational Modeling, Siberian Division, Russian Academy of Sciences, Krasnoyarsk 660036.
Translated from Prikladnaya Mekhanika i Tekhnicheskaya Fizika, Vol. 45, No. 1, pp. 29–38, January–February, 2004. Original article submitted December 30, 2002; revision submitted August 5, 2003.

$$f_t + (\boldsymbol{w} + \beta\chi\nabla\theta) \cdot \nabla f = 0; \tag{1.7}$$

$$[p_{\text{gas}} - \rho_0 q - \beta\chi\rho_0(\nu - \chi)\Delta\theta]\boldsymbol{n} + 2\rho_0\nu[D(\boldsymbol{w}) + \beta\chi D(\nabla\theta)]\boldsymbol{n} = 2\sigma(\theta)H\boldsymbol{n} + \nabla_{11}\sigma; \tag{1.8}$$

$$k\,\frac{\partial\theta}{\partial n} + b(\theta - \theta_{\text{gas}}) = Q. \tag{1.9}$$

Equation (1.7) is the kinematic condition, Eq. (1.8) is the dynamic condition, and Eq. (1.9) defines heat transfer between the liquid and gas medium, which is assumed to be passive ($k$ is the thermal conductivity, $b \geqslant 0$ is the heat-transfer coefficient, and $Q$ is the heat flux). In (1.8) and (1.9), $p_{\text{gas}}$ and $\theta_{\text{gas}}$ are the pressure and temperature specified in the gas (below, $p_{\text{gas}}$ and $\theta_{\text{gas}}$ are constants); $\boldsymbol{n} = \nabla f/|\nabla f|$ is the external normal to $S$; $\sigma(\theta)$ is approximated by the linear dependence

$$\sigma(\theta) = \sigma_1 - æ(\theta - \theta_1), \tag{1.10}$$

where $\sigma_1$ and $\theta_1$ are the surface tension and temperature at a certain point of $S$, $H$ is the mean curvature, and $\nabla_{11} = \nabla - \boldsymbol{n}(\boldsymbol{n} \cdot \nabla)$ is the surface gradient.

Further on, the free boundary has no common points with the solid wall; therefore, the conditions on the contact line are not considered (see [3, 4]).

**Remark.** In particular problems, the vector $\boldsymbol{g}$ either depends on time only or is $\boldsymbol{g} = \text{const}$. In these cases, the substitution (analog of the substitution of pressure by modified pressure in the Oberbeck–Boussinesq model)

$$q = \bar{q} + \boldsymbol{g}(t) \cdot \boldsymbol{x} \tag{1.11}$$

allows one to transform the right side of the momentum equation (1.1) to

$$(1 + \beta\theta)(-\nabla\bar{q} + \nu\Delta\boldsymbol{w}) - \beta\theta\boldsymbol{g}.$$

In the boundary condition (1.8), the expression $-\rho_0 q$ is replaced by $-\rho_0\bar{q} - \rho_0\boldsymbol{g}(t) \cdot \boldsymbol{x}$.

We have $\boldsymbol{g} = (0, 0, -g)$, where $g = \text{const} > 0$, everywhere below. It can be readily verified that the fluid can be in equilibrium [2] in the layer $0 < z < l$, $|x|, |y| < \infty$; the upper boundary of the layer is free, and the lower boundary $z = 0$ is the solid wall. The equilibrium state is as follows (the subscript 0 indicates the equilibrium position):

$$\begin{gathered}\boldsymbol{w}_0 = (0, 0, -\beta\chi\theta_{01}), \quad \theta_0(z) = \theta_{00} + \theta_{01}z, \quad q_0 = -g\ln[1 + \beta\theta_0(z)]/(\beta\theta_{01}) + c_1, \\ \theta_{01} = [Q + b(\theta_{\text{gas}} - \theta_{00})]/(k + bl), \qquad c_1 = p_{\text{gas}}/\rho_0 + g\ln[1 + \beta\theta_0(l)]/(\beta\theta_{01}).\end{gathered} \tag{1.12}$$

Here, $\theta_{00} = \text{const}$ is the temperature of the solid wall; without losing generality, we assume that $\theta_{00} = 0$. Thus, formulas (1.12) yield the exact solution of problem (1.1)–(1.3), (1.6)–(1.10) with a flat free boundary $z = l$. In contrast to the classical case, the function $q_0(z)$ (analog of pressure) here is distributed by the logarithmic rather than the linear law.

From (1.12), for $\beta \to 0$ and other parameters being fixed, we obtain

$$\boldsymbol{w}_0 = 0, \qquad \theta_0 = \theta_{01}z, \qquad q_0 = p_{\text{gas}}/\rho_0 + gl - gz. \tag{1.13}$$

Since the pressure is $p_0 = \rho_0 q_0$, Eq. (1.13) is the equilibrium state of the layer of a viscous heat-conducting fluid. This is not surprising because, by virtue of substitution (1.4), system (1.1)–(1.3) approximates the Navier–Stokes equations for such a fluid.

Retaining now second-order terms with respect to $\beta$ in expression (1.12) for $q_0(z)$ and denoting the deviation of pressure from the hydrostatic value as $\bar{p}_0(z) = \rho_0\bar{q}_0(z)$ [$\bar{q}_0(z) = q_0(z) + gz$ in accordance with substitution (1.11)], we obtain the equilibrium state of the flat layer in the Oberbeck–Boussinesq model [5]

$$\boldsymbol{w}_0 = 0, \quad \theta_0(z) = \theta_{01}z, \quad \bar{p}_0 = p_{\text{gas}} + \rho_0 g\beta[\theta_0^2(z) - \theta_0^2(l)]/(2\theta_{01}). \tag{1.14}$$

The equality for $\bar{p}_0(z)$ is usually written as

$$\frac{d\bar{p}_0}{dz} = \rho_0 g\beta\theta_0(z).$$

In this case, model (1.1)–(1.3), with allowance for the above-made comment, approximates the Oberbeck–Boussinesq model. It suffices to use $\beta = 0$ everywhere except for the expression $-\beta\theta\boldsymbol{g}$.

The equilibrium state (1.12) is studied below for stability by the linear approximation.

**2. Small Perturbations.** Equations of small perturbations for arbitrary solutions of the problem with a free boundary (1.1)–(1.3), (1.5)–(1.9) were obtained in [2]. Here, we specify them for the equilibrium state (1.12). Let $\boldsymbol{U}(\boldsymbol{x},t) = (U,V,W)$, $T(\boldsymbol{x},t)$, and $Q(\boldsymbol{x},t)$ be the perturbations of the basic equilibrium state $\boldsymbol{w}_0$, $\theta_0$, $q_0$ (1.12). We introduce the dimensionless variables

$$\boldsymbol{x}' = \frac{\boldsymbol{x}}{l}, \quad t' = \frac{\nu t}{l^2}, \quad \boldsymbol{U}' = \frac{l\boldsymbol{U}}{\nu}, \quad T' = \frac{T}{\mu\theta_{01} l \,\mathrm{Pr}}, \quad Q' = \frac{l^2 Q}{\nu^2}, \tag{2.1}$$

where $\mu = 1$ for $\theta_{01} > 0$ and $\mu = -1$ for $\theta_{01} < 0$.

Substituting (2.1) into (1.1)–(1.3), (1.5)–(1.9), we obtain the following problem of small perturbations in dimensionless variables (the primes are omitted):
— for $-\infty < x < \infty$, $-\infty < y < \infty$, and $0 < z < 1$,

$$U_t - \mu\varepsilon W_x/\mathrm{Pr} - \mu\varepsilon^2 T_{xz}/\mathrm{Pr} = (1+\mu\varepsilon z)(-Q_x + \Delta U), \tag{2.2}$$

$$V_t - \mu\varepsilon W_y/\mathrm{Pr} - \mu\varepsilon^2 T_{yz}/\mathrm{Pr} = (1+\mu\varepsilon z)(-Q_y + \Delta V), \tag{2.3}$$

$$W_t - \mu\varepsilon W_z/\mathrm{Pr} + \mu\varepsilon^2 (T_{xx} + T_{yy})/\mathrm{Pr} = (1+\mu\varepsilon z)(-Q_z + \Delta W) + \mathrm{Ra}/(1+\mu\varepsilon z), \tag{2.4}$$

$$T_t + \mu\varepsilon T_z/\mathrm{Pr} + \mu W/\mathrm{Pr} = (1+\mu\varepsilon z)\Delta T/\mathrm{Pr}, \tag{2.5}$$

$$U_x + V_y + W_z = 0; \tag{2.6}$$

on the free boundary $z = 1$,

$$\gamma R/(1+\mu\varepsilon) - Q + \varepsilon(1/\mathrm{Pr} - 1)\Delta T + 2W_z + 2\varepsilon T_{zz} = \mathrm{We}(R_{xx} + R_{yy}), \tag{2.7}$$

$$U_z + 2\varepsilon T_{xz} + W_x = -\mathrm{M}(T + \mu R/\mathrm{Pr})_x, \tag{2.8}$$

$$V_z + 2\varepsilon T_{yz} + W_y = -\mathrm{M}(T + \mu R/\mathrm{Pr})_y, \tag{2.9}$$

$$T_z + \mathrm{B}(T + \mu R/\mathrm{Pr}) = 0, \tag{2.10}$$

$$R_t = W + \varepsilon T_z; \tag{2.11}$$

on the solid wall $z = 0$,

$$U + \varepsilon T_x = 0, \quad V + \varepsilon T_y = 0, \quad W + \varepsilon T_z = 0, \quad T = 0; \tag{2.12}$$

— for $t = 0$,

$$\begin{gathered} U = U_1(x,y,z), \quad V = V_1(x,y,z), \quad W = W_1(x,y,z), \\ T = T_1(x,y,z), \qquad R = R_0(x,y), \qquad U_{1x} + V_{1y} + W_{1z} = 0. \end{gathered} \tag{2.13}$$

The following notation is introduced in problem (2.2)–(2.13): $\varepsilon = \mu\theta_{01} l\beta > 0$ is the Boussinesq parameter, $\mathrm{Pr} = \nu/\chi$ is the Prandtl number, $\mathrm{Ra} = \mu\theta_{01} l^4 \beta g/(\nu\chi) \equiv \varepsilon\eta$ is the Rayleigh number, where $\eta = gl^3/(\nu\chi)$ is the microconvection parameter [1], $\gamma = gl^3/\nu^2 = \eta/\mathrm{Pr}$ is the Galileo number, $\mathrm{We} = \sigma(\theta_0(l))l/(\rho_0\nu^2)$ is the modified Weber number, $\mathrm{M} = \mu æ \theta_{01} l^2/(\rho_0\nu\chi)$ is the Marangoni number, and $\mathrm{B} = bl/k$ is the Biot number.

The function $R(x,y,t)$ describes the perturbation of the free boundary $z = 1$, i.e., the deviation along the normal from this plane at each point.

We seek the solution of problem (2.2)–(2.12) in the form of normal waves

$$(\boldsymbol{U}, Q, T, R) = (\boldsymbol{U}(z), Q(z), T(z), R)\exp[i(\alpha_1 x + \alpha_2 y - Ct)], \tag{2.14}$$

where $\alpha_1$ and $\alpha_2$ are the dimensionless wave numbers along the $x$ and $y$ axes, respectively, and $C$ is the complex decrement determining the time evolution of the disturbance. The initial data (2.13) can be ignored. Substitution of (2.14) into (2.2)–(2.12) yields a homogeneous problem with respect to $U$, $V$, $W$, $Q$, $T$, $R$, which can be subjected to the Squire transformation [6]. Namely, if we assume that $Z = \alpha_1 U + \alpha_2 V$ and $k^2 = \alpha_1^2 + \alpha_2^2$, we obtain the following boundary-value problem for $Z$, $W$, $Q$, $T$, $R$, and the parameter $C$:
for $0 < z < 1$,

$$-iCZ - i\mu\varepsilon k^2 W/\mathrm{Pr} - i\mu\varepsilon^2 k^2 T'/\mathrm{Pr} = (1+\varepsilon\mu z)(Z'' - k^2 Z - ik^2 Q); \tag{2.15}$$

$$-iCW - \mu\varepsilon W'/\Pr - \mu\varepsilon^2 k^2 T/\Pr = (1+\varepsilon\mu z)(W'' - k^2 W - Q') + \mathrm{Ra}\, T/(1+\varepsilon\mu z); \tag{2.16}$$

$$-iCT + \mu\varepsilon T'/\Pr + \mu W/\Pr = (1+\varepsilon\mu z)(T'' - k^2 T)/\Pr; \tag{2.17}$$

$$iZ + W' = 0; \tag{2.18}$$

for $z = 1$,

$$-Q + \gamma R/(1+\mu\varepsilon) + 2W' + \varepsilon(1 + 1/\Pr)T'' + \varepsilon k^2(1 - 1/\Pr)T = -\mathrm{We}\, k^2 R; \tag{2.19}$$

$$Z' + 2i\varepsilon k^2 T' + ik^2 W = -i\mathrm{M}k^2(\mu R/\Pr + T); \tag{2.20}$$

$$T' + \mathrm{B}(T + \mu R/\Pr) = 0; \tag{2.21}$$

$$-iCR = W + \varepsilon T'; \tag{2.22}$$

for $z = 0$,

$$Z = T = 0, \qquad W + \varepsilon T' = 0. \tag{2.23}$$

The prime here denotes differentiation with respect to $z$.

**3. Long Waves.** We find the asymptotic behavior of the spectral problem (2.15)–(2.23) as $k \to 0$. We assume that

$$Z = Z_0 + k^2 Z_1 + \ldots, \quad W = W_0 + k^2 W_1 + \ldots, \quad Q = Q_0 + k^2 Q_1 + \ldots,$$

$$T = T_0 + k^2 T_1 + \ldots, \quad C = C_0 + k^2 C_1 + \ldots, \quad R = R_0 + k^2 R_1 + \ldots .$$

In the zero approximation, we obtain the problem

$$\begin{gathered} -iC_0 Z_0 = (1+\varepsilon\mu z)Z_0'', \\ -iC_0 W_0 - \mu\varepsilon W_0'/\Pr = (1+\varepsilon\mu z)(W_0'' - Q') + \mathrm{Ra}\, T_0/(1+\varepsilon\mu z), \\ -iC_0 T_0 + \mu\varepsilon T_0'/\Pr + \mu W_0/\Pr = (1+\varepsilon\mu z)T_0''/\Pr, \\ iZ_0 + W_0' = 0 \qquad (0 < z < 1); \end{gathered} \tag{3.1}$$

$$\begin{gathered} -Q_0 + \gamma R_0/(1+\mu\varepsilon) + \varepsilon(1 + 1/\Pr)T_0'' = 0, \\ Z_0' = 0, \qquad \mu \Pr T_0' + \mathrm{B}(\mu \Pr T_0 + R_0) = 0, \\ -iC_0 R_0 = W_0 + \varepsilon T_0' \qquad (z = 1); \end{gathered} \tag{3.2}$$

$$Z_0 = W_0 = T_0 = 0, \qquad W_0 + \varepsilon T_0' = 0 \qquad (z = 0). \tag{3.3}$$

Clearly, the spectral parameter $C_0$ is determined from the boundary-value problem for $Z_0$. Since

$$iC_0 \int\limits_0^1 \frac{|Z_0|^2}{1+\varepsilon\mu z}\, dz = \int\limits_0^1 |Z_0'|^2\, dz,$$

then, $C_0$ is a purely imaginary number, and $iC_0 > 0$. The value of $C_0$ can be easily refined. For this purpose, we introduce a new variable $s = 1 + \varepsilon\mu z$, then, $sZ_{0ss} + d^2 Z_0 = 0$, $Z_0(1) = Z_0'(s_1) = 0$, $s_1 = 1 + \varepsilon\mu$, $d^2 = iC/\varepsilon^2 > 0$. The equation for $Z_0(s)$ has the general solution

$$Z_0 = \sqrt{s}\,[h_1 J_1(2d\sqrt{s}) + h_2 J_1(2d\sqrt{s}\,)], \qquad h_1, h_2 = \mathrm{const},$$

where $J_1$ and $Y_1$ are the Bessel functions of the first and second kind. The boundary conditions for $Z_0$ show that $\tau = 2d$ is the root of the transcendental equation

$$J_1(\tau)Y_0(\tau\sqrt{s_1}) - Y_1(\tau)J_0(\tau\sqrt{s_1}) = 0, \tag{3.4}$$

which has a denumerable number [7] of real roots $\tau_n$. Therefore,

$$iC_{0n} = \varepsilon^2 \tau_n^2/4, \qquad n = 1, 2, \ldots . \tag{3.5}$$

Thus, long-wave perturbations decay monotonically regardless of the sign of $\theta_{01}$.

**4. Layer of a Viscous Heat-Conducting Fluid.** In this case, we have $\varepsilon = 0$ ($\beta = 0$), and problem (2.15)–(2.23) is simplified to

$$-iCZ = Z'' - k^2Z - ik^2Q, \qquad -iCW = W'' - k^2W - Q',$$
$$-iC\,\mathrm{Pr}\,T + \mu W = T'' - k^2T, \qquad iZ + W' = 0 \qquad (0 < z < 1); \tag{4.1}$$

$$-Q + \gamma R + 2W' = -\,\mathrm{We}\,k^2R, \qquad Z' + ik^2W = -ik^2\mathrm{M}(\mu R/\,\mathrm{Pr}\, + T),$$
$$T' + \mathrm{B}(\mu R/\,\mathrm{Pr}\, + T) = 0, \qquad -iCR = W \qquad (z = 1); \tag{4.2}$$

$$Z = W = T = 0 \qquad (z = 0). \tag{4.3}$$

System (4.1) has the general solution

$$Z = id(b_1\cos dz - b_2\sin dz) + ik^2(a_1\sinh\,kz + a_2\cosh\,kz)/(k^2 + d^2),$$
$$W = b_1\sin dz + b_2\cos dz + k(a_1\cosh\,kz + a_2\sinh\,kz)/(k^2 + d^2),$$
$$Q = a_1\sinh\,kz + a_2\cosh\,kz, \tag{4.4}$$
$$T = h_1\sin qz + h_2\cos qz + \frac{\mu b_1\sin dz}{q^2 - d^2} + \frac{\mu b_2\cos dz}{q^2 - d^2} + \frac{k\mu}{(k^2 + d^2)(k^2 + q^2)}(a_1\cosh\,kz + a_2\sinh\,kz),$$

where $a_1$, $a_2$, $b_1$, $b_2$, $h_1$, and $h_2$ are constants, $q^2 = iC\,\mathrm{Pr} - k^2$, and $d^2 = iC - k^2$ ($\mathrm{Pr} \neq 1$).

Let $iC = \tau$, then $q^2 + k^2 = \tau\,\mathrm{Pr}$, $k^2 + d^2 = \tau$, $q^2 - d^2 = (\mathrm{Pr} - 1)\tau$, and from the boundary conditions (4.3), we obtain

$$b_1 = -\frac{k^2a_2}{d\tau}, \qquad b_2 = -\frac{ka_1}{\tau}, \qquad h_2 = \frac{k\mu a_1}{\tau^2\,\mathrm{Pr}(\mathrm{Pr} - 1)}. \tag{4.5}$$

Since $R = -W/\tau$, conditions (4.2) on the free boundary $z = 1$ reduce to the following ($\mu^2 = 1$):

$$2W' - Q - (\gamma + k^2\,\mathrm{We})W/\tau = 0,$$
$$Z' + ik^2W + i\mu k^2\mathrm{M}(\mu T - W/(\tau\,\mathrm{Pr})) = 0, \qquad \mu\,\mathrm{Pr}\,T' + \mathrm{B}(\mu\,\mathrm{Pr}\,T - W/\tau) = 0. \tag{4.6}$$

System (4.6) together with (4.5) allows one to determine the complex decrement $C$ for $\mathrm{Pr} \neq 1$. Nevertheless, the corresponding characteristic determinant is extremely complicated, and problem (4.1)–(4.3) for $\gamma = 0$ was solved in [8] by a numerical (orthogonalization) method. Here, we present the dependence of the Marangoni number for $\gamma \neq 0$ for monotonic perturbations, where $C = 0$. The computations show that

$$\mathrm{M} = -\frac{8\mu k(k - \sinh\,k\cosh\,k)(k\cosh\,k + \mathrm{B}\sinh\,k)}{k^3\cosh\,k - \sinh^3 k - 8k^5\cosh\,k\,\mathrm{Pr}^{-1}(\gamma + k^2\,\mathrm{We})^{-1}}. \tag{4.7}$$

For $\gamma = 0$, this expression coincides with than obtained in [8]. From (4.7), for small $k$, we have

$$\mathrm{M} \sim -2\mu\gamma\,\mathrm{Pr}(\mathrm{B} + 1)/3. \tag{4.8}$$

If we perform similar transformations for the Oberbeck–Boussinesq model, then instead of (4.8), we obtain

$$\mathrm{M} \sim -(2/3)\mu\gamma\,\mathrm{Pr}(\mathrm{B} + 1) - (11/60)\,\mathrm{B}\,\mathrm{Ra}, \tag{4.9}$$

where Ra is the Rayleigh number. Note, for heating from below ($\mu = -1$), we have $\mathrm{Ra} \leqslant 40\gamma(\mathrm{B} + 1)/(11\,\mathrm{B}) = \mathrm{Ra}_*$, and there is no neutral curve for $\mathrm{Ra} > \mathrm{Ra}_*$. For $\mathrm{B} \to \infty$, the limiting value of $\mathrm{Ra}_*$ coincides with that calculated in [9] for $\mathrm{M} = 0$. The case $\mathrm{B} = \infty$ indicates that the temperature rather than the heat exchange with the ambient medium is set on the free surface.

**5. Analysis of Numerical Results.** First, we note that the Boussinesq parameter, Rayleigh number, and Marangoni number are proportional to each other, since they depend on a controlled parameter: temperature gradient $\theta_{01}$. Therefore, it is convenient to introduce new parameters $\alpha = \rho_0\nu\beta\chi/(æl)$ and $\Gamma = \rho_0\beta gl^2/\chi$ (then, $\varepsilon = \alpha\mathrm{M}$ and $\mathrm{Ra} = \Gamma\mathrm{M} = \mathrm{Pr}\,\alpha\gamma\mathrm{M}$) and determine the Marangoni number. For the Oberbeck–Boussinesq model, stability of the layer with a linear dependence of Ra and M was considered in [10–12].

The numerical solution of problem (2.15)–(2.23) for arbitrary perturbations was performed by the method of orthogonalization. Expression (4.7) was used as a test in numerical construction of the neutral curves. The

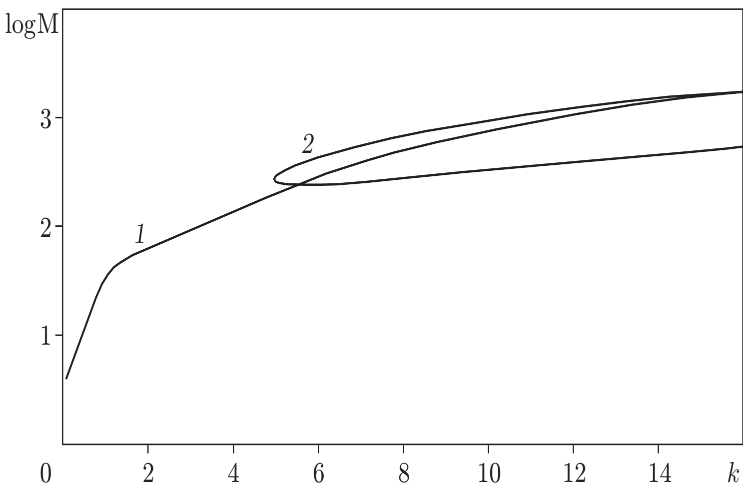


Fig. 1

TABLE 1

| $\alpha$ | $\gamma$ | $M_*$ | $k_*$ |
|---|---|---|---|
| 0 | 0 | 224.93 | 5.35 |
| 0 | $10^3$ | 226.51 | 5.35 |
| $10^{-4}$ | 0 | 230.88 | 5.50 |
| $10^{-4}$ | $10^3$ | 232.47 | 5.50 |

TABLE 2

| $\gamma$ | $M_{*1}$ | $M_{*2}$ | $M_{*3}$ | $M_{*4}$ | $M_{*5}$ |
|---|---|---|---|---|---|
| $10^6$ | 74.3 | 739.3 | 362.7 | 8032 | 9825.6 |
| $10^7$ | 49.1 | 2357 | 767.3 | 3214.5 | 6122 |

calculation results for $\alpha = 0$ and $\Gamma \neq 0$ coincide with the numerical data of [10] obtained within the framework of the Oberbeck–Boussinesq model.

Figure 1 shows the neutral curves constructed for $\gamma = 10^3$, $\mathrm{Pr} = 5.41 \cdot 10^{-3}$, $\mathrm{We} = 10^4$, and $\alpha = 10^{-4}$. Curves 1 and 2 correspond to monotonic and oscillatory perturbations, respectively. The asymptotic equations (3.5) and (4.9) were used for numerical construction of the neutral curve 2. In Fig. 1, the region of stability to monotonic perturbations is above curve 1, and the region of stability to oscillatory perturbations lies inside curve 2.

The conducted calculations showed that, for low values of the parameters $\alpha$ and $\Gamma$, the qualitative behavior of the neutral curves coincides with the behavior of the corresponding curves for a viscous heat-conducting fluid ($\alpha = 0$, $\gamma = 0$) [8]. As was found in [8], curve 1 corresponds to thermocapillary perturbations associated with nonuniform heating of the fluid, and curve 2 indicates the boundary of stability to capillary perturbations induced by free boundary deformations.

For some values of $\alpha$ and $\gamma$, Table 1 gives the minimum values $M_*$ of the capillary neutral curve (curve 2) and the values of the wavenumber $k_*$ at which these minimums are reached. Thus, allowance for compressibility of the fluid ($\alpha \neq 0$) leads to stabilization of capillary perturbations; even for low values of the parameter $\alpha$, the values of the critical Marangoni numbers can be significantly different.

Another specific feature of the model under consideration is the emergence (with increasing influence of gravity forces) of new neutral curves, caused by allowance for fluid compressibility. In Fig. 2 constructed for $\gamma = 10^6$, $\mathrm{Pr} = 5.41 \cdot 10^{-3}$, $\mathrm{We} = 10^4$, and $\alpha = 10^{-4}$, these new neutral curves are denoted as 3–5, whereas curves 1 and 2 are the same as in Fig. 1. Perturbations corresponding to the new mechanism of instability increase monotonically, and the region of instability is located above the corresponding neutral curve. As is shown in Fig. 3 constructed for $\gamma = 10^7$, an increase in the gravity force leads to further stabilization of capillary perturbations, and the threshold of stability for thermocapillary perturbations and new perturbations caused by fluid compressibility decreases. The minimum values $M_{*j}$ corresponding to the $j$th neutral curves in Figs. 2 and 3 are listed in Table 2.

Figure 4 constructed for $\gamma = 10^7$, $\mathrm{M} = 3400$, $\mathrm{Pr} = 5.41 \cdot 10^{-3}$, $\mathrm{We} = 10^4$, and $\alpha = 10^{-4}$ shows the behavior of the complex decrement of the problem as a function of the wavenumber. Curves 1 and 2 here refer to the thermocapillary monotonic and capillary oscillatory modes, respectively. Curves 3 and 4 refer to new perturbations caused by fluid compressibility. The eigenvalues of the problem corresponding to the neutral curve 5 (in Figs. 2 and 3) lie in the negative half-plane and are not shown in Fig. 4.

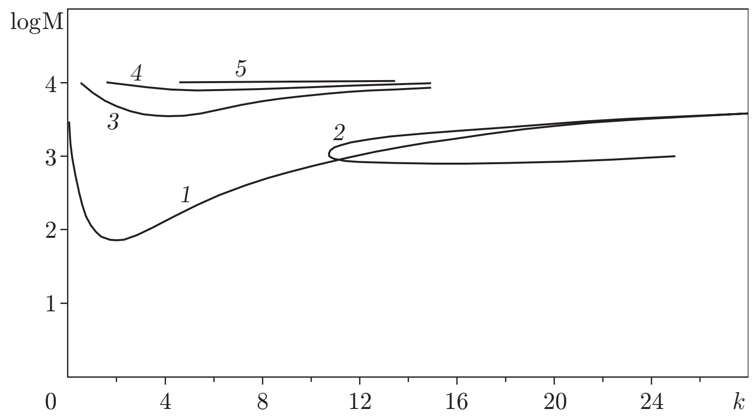


Fig. 2

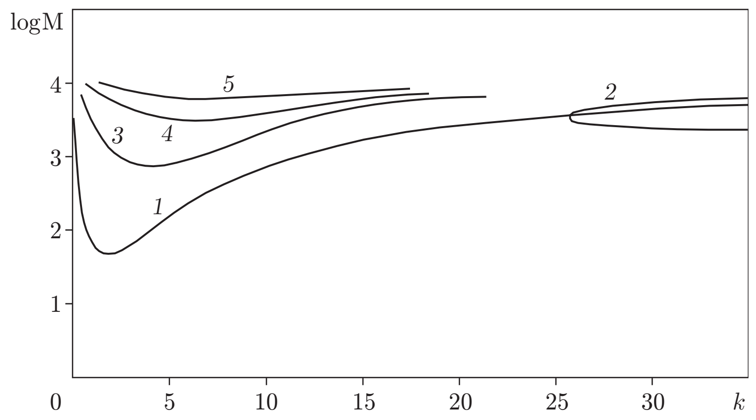


Fig. 3

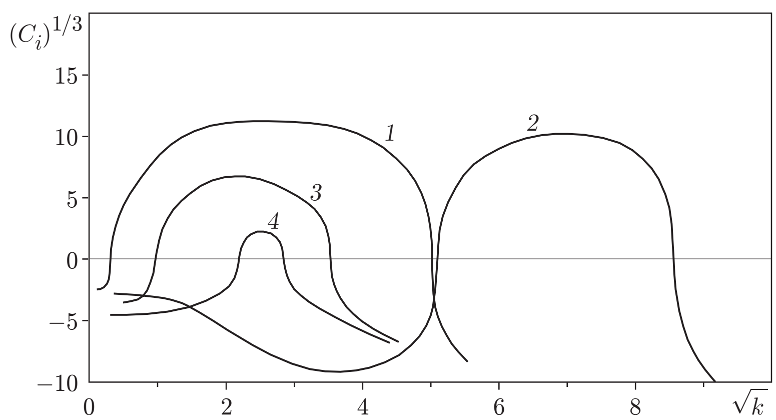


Fig. 4

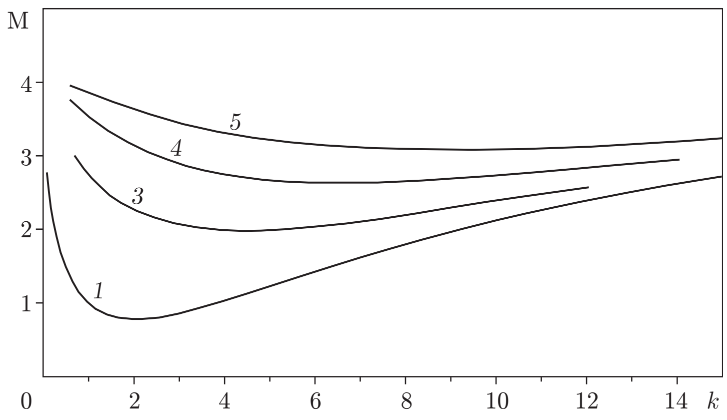


Fig. 5

TABLE 3

| We | $M_{*1}$ | $M_{*2}$ | $M_{*3}$ | $M_{*4}$ | $M_{*5}$ |
|---|---|---|---|---|---|
| $10^2$ | 74.3 | 209.8 | 361.3 | 8032 | 9825.6 |
| $10^6$ | 74.6 | — | 373.4 | 8165.6 | 9831.7 |

The effect of increasing Prandtl number on equilibrium stability is illustrated in Fig. 5 constructed for $\gamma = 10^6$, Pr = 1, We = $10^4$, and $\alpha = 10^{-4}$ (the neutral curves are enumerated in the same manner as in the previous figures). The figure does not show the neutral curve for capillary perturbations. With increasing Prandtl number, the region of instability is shifted toward very short waves, and the minimum value of the Marangoni number substantially increases. An increase in Prandtl number leads to significant destabilization of monotonic perturbations. The threshold of stability decreases for all perturbations. Thus, with respect to thermocapillary perturbations, the loss of stability occurs already at M = 6.2.

The effect of deformability of the free boundary on equilibrium stability is illustrated by Table 3 composed for $\gamma = 10^6$, $\mathrm{Pr} = 5.41 \cdot 10^{-3}$, and $\alpha = 10^{-4}$. As the Weber number decreases, the threshold of stability to capillary perturbations significantly decreases; correspondingly, as We increases, stability to these perturbations is stabilized. There is no capillary instability altogether at We = $10^6$. For monotonic perturbations, the changes in the Weber number have almost no effect on the threshold of stability.

Based on the above-described results, we can conclude that thermocapillary perturbations are most dangerous in a wide range of problem parameters, whereas oscillatory capillary perturbations dominate in the range of very short waves for moderate values of Pr and We.

The areas of applicability of the microconvection, Oberbeck–Boussinesq, and viscous heat-conducting fluid models in the considered problem of equilibrium stability (1.12) are estimated. The influence of buoyancy forces was studied for fixed values $\alpha = 10^{-4}$, $\mathrm{Pr} = 5.41 \cdot 10^{-3}$, and We = $10^4$. As a criterion, we used the relation $\min\limits_k (|\mathrm{M}(k) - \mathrm{M}_t(k)|/\mathrm{M}(k)) \leqslant 0.05$, where $\mathrm{M}_t(k)$ is the neutral curve constructed within the framework of the model of a viscous heat-conducting fluid ($\alpha = 0$). The calculations showed that the allowance for buoyancy forces leads to significant differences in the Marangoni number (greater than 5%) for $\gamma = 8 \cdot 10^5$. The relative error in finding the critical Marangoni number decreases with decreasing $\gamma$.

In studying compressibility of the fluid, the criterion was the relation

$$\min_k (|\mathrm{M}(k) - \mathrm{M}_b(k)|/\mathrm{M}(k)) \leqslant 0.05,$$

where $\mathrm{M}_b(k)$ is the neutral curve constructed by the Oberbeck–Boussinesq model ($\alpha = 0$ and $\Gamma \neq 0$). The calculations were performed for $\gamma = 10^4$, $\mathrm{Pr} = 5.41 \cdot 10^{-3}$, and We = $10^4$. It is shown that the allowance for compressibility starts to play a noticeable role for $\alpha > 2 \cdot 10^{-4}$. Here, the relative error also decreases with decreasing $\alpha$.

This work was supported by the Russian Foundation for Fundamental Research (Grant No. 02-01-10087) and within the framework of the Integration Project No. 131 of the Siberian Division of the Russian Academy of Sciences.

**REFERENCES**


1. V. V. Pukhnachev, “Model of convective motion under reduced gravity,” *Model. Mekh.*, **6**, No. 4, 47–56 (1992).
2. V. K. Andreev and V. B. Bekezhanova, “Emergence of microconvection in a flat layer,” Preprint No. 1-01, Inst. Computational Modeling, Sib. Div., Russian Acad. of Sci., Krasnoyarsk (2001).
3. V. V. Pukhnachev and V. A. Solonnikov, “Dynamic contact angle,” *Prikl. Mat. Mekh.*, **46**, No. 6, 961–971 (1982).
4. V. V. Pukhnachev, *Motion of a Viscous Fluid with Free Boundary: Teaching Aid* [in Russian], Novosibirsk State Univ., Novosibirsk (1989).
5. G. Z. Gershuni and E. M. Zhukhovitskii, *Convective Stability of an Incompressible Fluid* [in Russian], Nauka, Moscow (1972).
6. A. S. Monin and A. M. Yaglom, *Statistische Hydromechanik.* 1. *Mechanik der Turbulenz*, Verlag–Nauka, Moskau (1965).
7. E. Jahnke, F. Emde, and Lösh, *Tafeln Hhërer Funktionen*, Teubuer, Stuttgart (1959).
8. E. A. Ryabitskii, “Thermocapillary instability of equilibrium of a flay layer with a vertical temperature gradient,” *Izv. Ross. Akad. Nauk, Mekh. Zhidk. Gaza*, No. 3, 19–23 (1992).
9. V. Kh. Izakson and V. I. Yudovich, “Origination of convection in a fluid layer with a free boundary,” *Izv. Akad. Nauk SSSR, Mekh. Zhidk. Gaza*, No. 4, 23–28 (1968).
10. I. Hashim and S. K. Wilson, “The onset of Benard–Marangoni convection in a horizontal layer of fluid,” *Int. J. Eng. Sci.*, **37**, 643–662 (1999).
11. R. D. Bengyria and M. C. Derassier, “On the linear stability of Benard–Marangoni convection,” *Phys. Fluids, A*, **1**, No. 7, 1123–1127 (1989).
12. C. Peter-Garcia and G. Carneiro, “Linear stability analysis of Benard–Marangoni convection in fluids with a deformable free surface,” *Phys. Fluids, A*, **3**, No. 2, 292–298 (1991).